

Relationship between Surface Slope, Average Facet Size, and Facet Flatness Tolerance of a Wind-Disturbed Water Surface

ALLEN H. SCHOOLEY

*U. S. Naval Research Laboratory
Washington 25, D. C.*

Abstract. Experimental relationships are given relating wind velocity to the parameters given in the title. Photographically obtained profiles of waves in a short-fetch water-wind tunnel were used as the source of data. The term 'roughness factor' is defined as the ratio of facet flatness tolerance to facet length. Average roughness factor increases with wind velocity in the region of near-zero facet slope. For facet slopes greater than about $+10^\circ$ and -10° , the situation is reversed. In this region, the average roughness factor is greater for positive slopes than for negative slopes.

Introduction. The dancing sparkles of sunlight reflected from the wind-swept surface of the sea have intrigued mankind from time immemorial. In recent years, considerable work has been done in determining details of the statistical distribution of surface slope for the variables of wind velocity and fetch. Experimental data taken by several observers on mean square slope as a function of local wind velocity for various fetches are summarized in Figure 1. The open-circle points represent measurements made in the Pacific Ocean [Cox and Munk, 1954], the crosses are for data taken on the Anacostia River [Schooley, 1954], and the rest are for laboratory measurements of the water surface at the lower boundary of a wind tunnel [Cox, 1958; Schooley, 1958]. The interesting thing about Figure 1 is the fact that, although the fetch covers a range of about $10^4:1$, the mean square slope varies only by about 2:1. Thus the short-fetch water-wind tunnel appears to be a practical device for obtaining significant information on at least one aspect of the phenomenon of wind-generated water waves.

Figure 2 shows sparkles of light being reflected from the randomly orientated 'facets' of a wind-disturbed water surface. Close examination reveals that the sparkles or facets are not all of the same size.

The reflection of light from the surface of the wind-swept sea is of considerable interest. Of importance, also, is the reflection of radar and sonar waves from the rough sea surface because such reflections are the source of unwanted signals called 'sea-clutter' in radar and 'surface

reverberation' in sonar. It is interesting to note that optical wavelengths are about 10^5 times smaller than the often-used radar and sonar wavelengths in the 1-cm to 10-cm region. No doubt Figure 2 would look quite different if it were possible to take the picture with illumination having a wavelength in the region of 1 to 10 cm instead of 4 to 7×10^{-5} cm. Experimentally, microwave radar sea-clutter has been closely associated with the local wind velocity [Schooley, 1956]. Hence, it may be assumed that the short-fetch water-wind tunnel will also be a practical device for obtaining significant oceanographic data in this region.

Experimental procedure. It is the purpose of

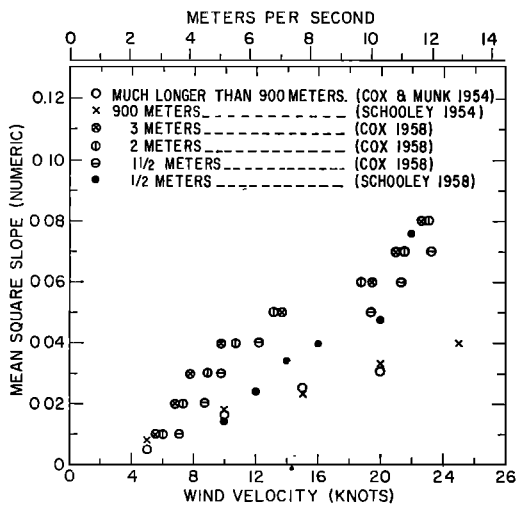


Fig. 1. Historical data on mean square slope versus wind velocity for various fetches.

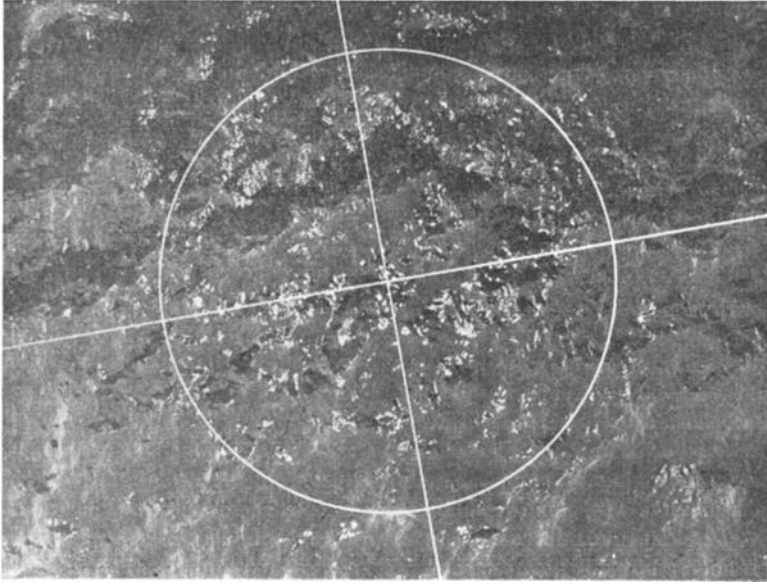


Fig. 2. Facets of light reflected from a wind-swept water surface.

this paper to present experimental data that show the relation of wind velocity to surface slope and facet size for various flatness tolerances. Flatness tolerance is defined in Figure 3. The heavy irregular line represents a water-wave profile with the wind blowing from left to right. The light solid line at an angle $-\theta$ with respect to the mean surface level is drawn tangent to one point on the wave profile and represents the slope at this point. Very short electromagnetic waves striking the surface at right angles to the tangent would be reflected back from a small facet of the water surface centered at this point. The size of the facet would be determined by its flatness, measured in terms of a fraction of a wavelength. In this paper, 'flatness tolerance' will be defined as $1/10$ of a wavelength. In Figure 3 flatness tolerances (a) and (b) are

indicated, together with the corresponding facet lengths. In the data to be presented, four flatness tolerances have been used: 1mm, 3mm, 5mm, and 10 mm, which correspond, by definition, to 1-cm, 3-cm, 5-cm, and 10-cm wavelengths.

Figure 4 shows the profile of a water wave created by a 16-knot wind blowing from left to right. The channel is about 10 cm wide and 70 cm long. This length corresponds to about 10^6 optical wavelengths and seven 10-cm wavelengths. In Figure 4 the boundary between the air, the water, and the front transparent wall of the channel has been retouched to make it more visible in the illustration. Full-size pictures similar to this were used in taking the experimental measurements. The slope and facet lengths for the chosen flatness tolerances were measured graphically at $1/2$ -cm intervals along

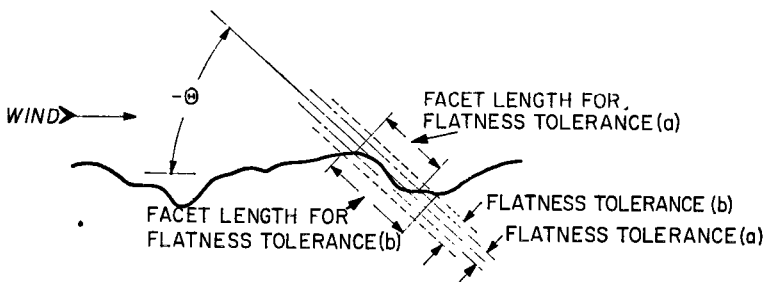


Fig. 3. Flatness tolerance used to determine facet length.

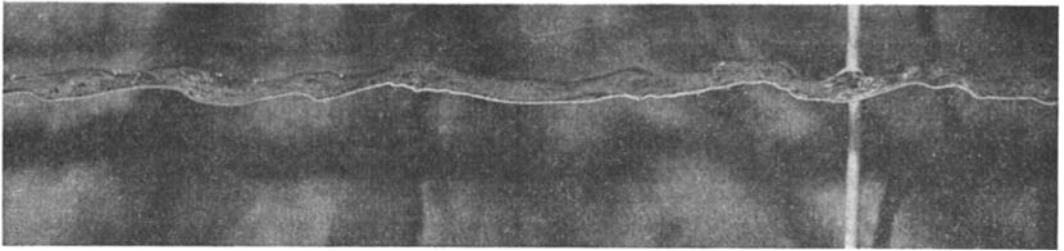


Fig. 4. Profile of a wave in a transparent water-wind tunnel.

many wave profiles for various wind velocities.

The results were plotted on a series of graphs similar to that shown in Figure 5. Facet length is the ordinate and slope is the abscissa. The points have a statistical scatter about the mean value which is shown by the curve. Similar plotting and averaging was done for various flatness tolerances and for various wind velocities.

Figure 6 shows the results for wind velocities of 10, 15, and 20 knots, and for a 1-mm flatness tolerance. Figures 7, 8, and 9 are similar except that the flatness tolerances are 3 mm, 5 mm, and 10 mm, respectively. The individual curves do not seem to be simple mathematical functions, and the families of curves are apparently not related by simple mathematical relationships. Empirical attempts to fit them empirically to statistical distribution formulas and to solutions of second-order differential equations led to much work and a not very precise fit.

It is difficult to estimate the total experimental errors that may enter into the presentations of the data given in Figures 6, 7, 8, and 9. First, there is the fact that the profiles of the waves at the channel boundary are not identical with what they would be away from the boundary. Visual examination of Figure 4 indicates that the difference is probably not serious. Next, the graphical determination of the facet length for various flatness tolerances introduces errors. Individual random errors probably largely balance out in the averaging process. However, the accuracy for the flatness tolerance of 1 mm is probably less than that for the 3- and 5-mm tolerances because of the smaller scale of the graphical measurements. Errors due to the finite length of the channel would tend to be larger for the 10-mm flatness tolerance than for the lesser flatness tolerances. Finally, statistical averaging errors depend upon the number of

points used in averaging is greater in the region around the 0° slope. Hence, the curves are probably more accurate in this region than for the larger slopes. There is one exception to this, however. The 10-knot curve in Figure 9 shows a break in the curve near the 0° slope because it tends to go to a very high value of average facet length. The accuracy in this region for this curve is not as great as that for the other curves, and the inaccuracy is related to the finite length of the water-wind tunnel.

Dimensional analysis. The following quantities, listed in three groups, appear to be involved in the phenomenon of wind-generated water waves.

Driving

(M) Air momentum

(η) Air viscosity

Restoring

(g) Gravity

(ρ_w) Water density

(T) Surface tension

Response

(s) Slope distribution

(R) Roughness factor =

$\frac{(l) \text{ flatness tolerance}}{(L) \text{ facet length}}$

The *driving* phenomenon is the velocity of the viscous air mass over the water surface. The weight of the water, which depends upon its

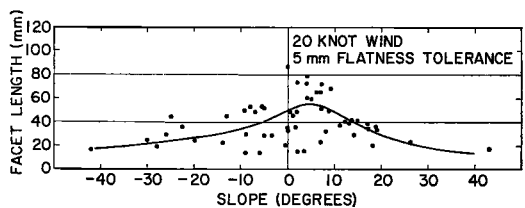


Fig. 5. Sample of statistical data.

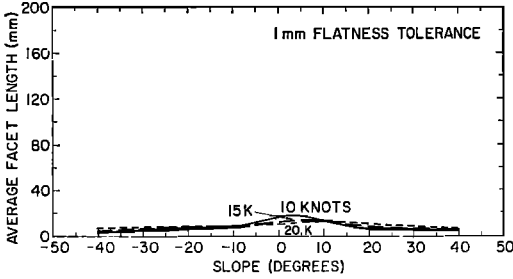


Fig. 6. Average facet length versus slope for 1-mm flatness tolerance.

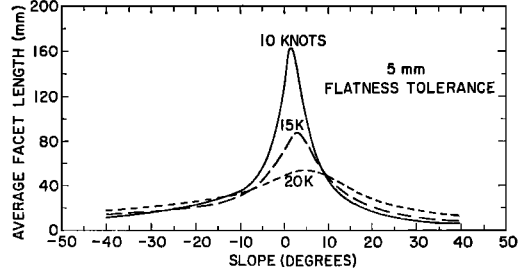


Fig. 8. Average facet length versus slope for 5-mm flatness tolerance.

density and the acceleration of gravity, and the surface tension tend to *restore* the surface to its mean level. The surface of the water *responds* to the wind by having a distribution of facet slopes and a distribution of facet sizes. As is noted in Figure 3, facet size depends upon the flatness tolerance used. For convenience we may define the term 'roughness factor' (R) as flatness tolerance divided by facet length.

Both slope distribution s and roughness factor R are dimensionless quantities that may be indicated as π_1 and π_2 , as shown below together with the quantity π_3 .

$$\pi_1 = (s) \tag{1}$$

$$\pi_2 = (R) \tag{2}$$

$$\pi_3 = \frac{g\rho_w M}{T\eta} \tag{3}$$

π_3 is an interesting dimensionless group because it incorporates all the other variables not included in π_1 and π_2 . Although it is possible that other dimensionless groups are important, we shall assume as an approximation that

$$\pi_1 = f(\pi_2, \pi_3) \tag{4}$$

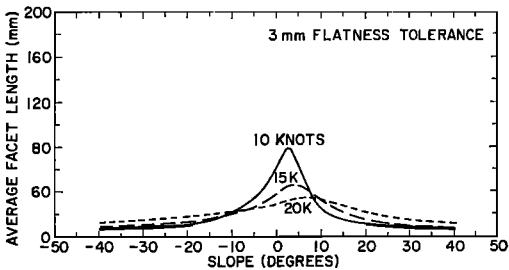


Fig. 7. Average facet length versus slope for 3-mm flatness tolerance.

Substituting the π values as given in (1), (2), and (3) yields

$$s = f\left(R, \frac{g\rho_w M}{T\eta}\right) \tag{5}$$

In the last term, air momentum may be expanded into more fundamental quantities, giving

$$s = f\left[R, \frac{g\rho_w \rho_a}{T\eta} (Fhw)\right] \tag{6}$$

where

- g is the acceleration of gravity.
- ρ_w is the density of the water.
- ρ_a is the density of the air.
- T is the surface tension of the water.
- η is the viscosity of the air.
- F is the fetch of the wind.
- h is the effective height of the wind.
- v is the wind velocity.

The first five of the above quantities may be considered constant as a first approximation. As indicated previously, fetch F is believed not to be

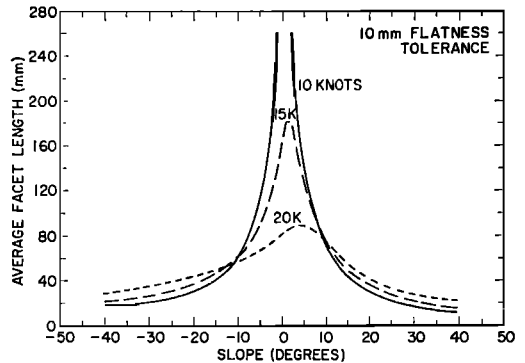


Fig. 9. Average facet length versus slope for 10-mm flatness tolerance.

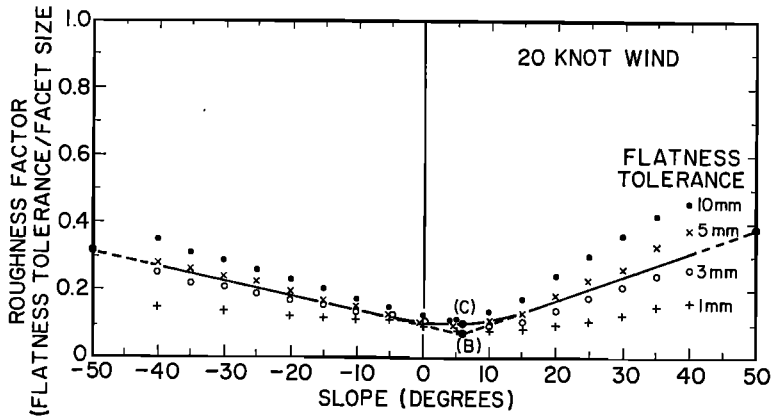


Fig. 10. Roughness factor versus slope, showing flatness tolerance points for 20-knot wind.

a major variable. In addition, it is a constant for the measurements described herein. The effective height of the wind is an interesting variable that is probably dependent to some extent on the wind velocity but is assumed to be constant for these experiments. Thus, it is again indicated that the velocity of the wind is the principal variable that influences the roughness and slope distributions of a wind-disturbed water surface.

Results. Figure 10 shows the experimental data for a wind velocity of 20 knots plotted with the dimensionless quantity, roughness factor, as ordinate and the slope, which is also dimensionless, as abscissa. The points for each of the four flatness tolerances are shown. The solid black curve is an average for all the points. The curve fits the 3-mm and 5-mm data fairly well. The fit

for the 1-mm and 10-mm data is not as good. It is evident that separate curves for each of the flatness tolerances could be drawn, but it is really not known whether this is proper because the 1-mm and 10-mm measurements are probably not as accurate as the 3-mm and 5-mm measurements, as was discussed previously.

The solid curve in Figure 10, although it does not fit all the data very closely, does have the merit of being relatively simple. To construct it, two straight lines are drawn between the convergent point *B* and the $+50^\circ$ and -50° roughness factor intercepts. The transition between the two straight lines is smoothed by drawing a gentle arc through the minimum point *C*. With this approximate and simplifying procedure, all the experimental data are gathered together in one graph (Fig. 11).

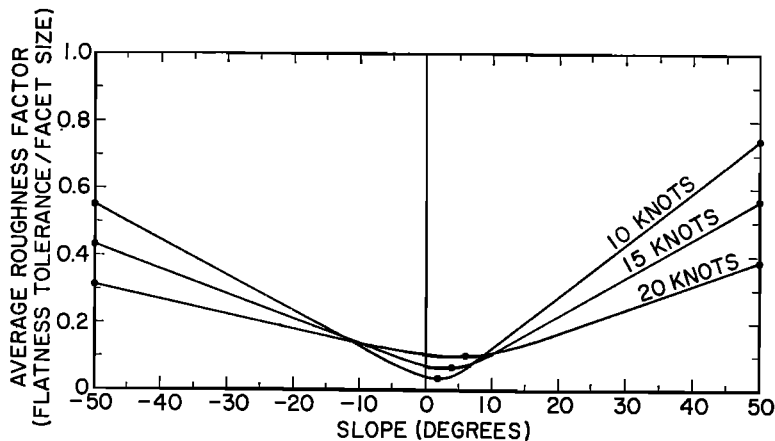


Fig. 11. Average roughness factor versus slope for various wind velocities.

It is interesting to note that the average roughness factor is greatest for the high wind velocities in the general region between the $+10^\circ$ and -10° surface slope. For slopes outside this general region, the situation is reversed. The points for minimum average roughness factor are greater and farther from the 0° slope axis for the higher wind velocities. For a given wind velocity, the curve is steeper on the positive-slope side than on the negative-slope side.

Discussion. Strictly speaking, the sea surface is continuous and is not made up of a distribution of facets having different sizes and slopes. However, this concept is useful because it leads to an explanation of some aspects of radar sea-clutter that have not been quantitatively interpreted before. *Katzin* [1957] showed the importance of facet size in the mechanisms of radar sea-clutter and also indicated that no measurements of facet size distribution existed. Although he made certain assumptions regarding the distribution of facet size, he was unable to develop the theory that explained the observed experimental fact that radar sea-clutter is considerably greater when the radar set is looking upwind than when looking downwind.

Preliminary calculations (not given in this paper) show that an upwind-downwind effect of about the right magnitude is obtained when the calculations are based on the experimental data contained in this paper.

REFERENCES

- Cox, C. S., Measurements of slopes of high-frequency wind waves, *J. Marine Research, Sears Foundation, 16*, 199-230, 1958.
- Cox, C. S., and W. H. Munk, Statistics of the sea surface derived from sun glitter, *J. Marine Research, Sears Foundation, 13*, 98-227, 1954.
- Katzin, Martin, On the mechanisms of radar sea clutter, *Proc. IRE, 45*, 44-54, 1957.
- Schooley, A. H., A simple optical method for measuring the statistical distribution of water surface slopes, *J. Opt. Soc. Am., 44*, 37-40, 1954.
- Schooley, A. H., Some limiting cases of radar sea clutter noise, *Proc. IRE, 44*, 1043-1047, 1956.
- Schooley, A. H., Probability distributions of water-wave slopes under conditions of short fetch, *Trans. Am. Geophys. Union, 39*, 405-408, 1958.

(Manuscript received September 1, 1960; revised October 26, 1960; presented at the Twelfth General Assembly of the International Union of Geodesy and Geophysics, Helsinki, Finland, July-August 1960.)